



Correlation Between XRF Data and Pigment Radiopacity

The x-ray absorption of paint matter (consequently grey levels directly measured on radiographic films) as well as the data obtained through XRF measurements on it depend on its chemical composition. First of all, the theoretical background was considered; then a series of reproducible standards were carried out and the calculated data for their x-ray absorption was compared with their grey levels (optical densities), measured directly on the x-ray films. In this way it was possible to evaluate the radiopacity of the pigments. The influence of thickness variability was taken into account. As an example, the model was applied to a painting by Antonello da Messina

■ *Pietro Moioli, Claudio Seccaroni*

Mass Absorption Coefficients and Reference Standards Preparation

The attenuation of a beam of x-radiation having an energy E which crosses a medium is given by

$$I = I_0 \exp[-\mu(E) \cdot t] = I_0 \exp[-S(E) \cdot x]$$

where I is the intensity of the incident beam, I_0 the intensity of the transmitted beam, $\mu(E)$ the mass absorption coefficient [cm^2/gr], $S(E)$ the linear absorption coefficient [cm^{-1}], t the thickness of the medium in gr/cm^2 , x its thickness in cm.

For all the chemical elements the absorption coefficients can be found tabulated as a function of the energy [1]. The absorption coefficients of any material having known composition can be calculated as

$$\mu(E) = c_1\mu_1(E) + \dots + c_n\mu_n(E)$$

$$S(E) = \mu(E)/\rho$$

where $\mu_1(E), \dots, \mu_n(E)$ are the absorption coefficients of the constitutive elements, c_1, \dots, c_n their concentrations, and ρ the density of the material.

In 1929, A. Martin de Wild calculated mass absorption coefficients for many pigments at the energy of about 15 keV [2]. For a group of these pigments, he also calculated the mass absorption coefficients taking into consideration the quantity of linseed oil required to form an adequate paint layer. This is the only known investigation concerning the calculation of the mass absorption coefficients of pigments. Conversely, more recent publications on the reading of x-radiographs of paintings generally report semi-quantitative evaluations of pigment mass absorption coefficients, where a few categories (such as low, medium, medium-high, high, very high) are individuated [3-5].

Therefore, the contribution of the paint layers to the attenuation of the x-beam may be calculated on the basis of their composition and of the energy of the x-radiation. The radiopacity of the paint layers (i.e., the capability to absorb the x-rays passing through them) depends on the mass absorption coefficient of the materials, which in turn depends on the atomic number of the chemical elements present, and then on the physical density of the materials as well as on the energy of the x-radiation [6]. Directly related to radiopacity, is the grey level of the corresponding area on the radiographic plate, also

■ **Pietro Moioli, Claudio Seccaroni**
 ENEA, Unità Tecnica Tecnologie dei Materiali

| | ρ | μ | S | R | σ |
|------------------|--------|-------|-------|-------|----------|
| titanium white | 2.19 | 34.50 | 15.75 | 1.043 | 0.207 |
| zinc white | 2.51 | 52.57 | 20.94 | 1.179 | 0.198 |
| yellow ochre | 1.58 | 8.02 | 5.08 | 0.576 | 0.390 |
| natural sienna | 1.46 | 10.36 | 7.10 | 0.416 | 0.235 |
| chrome yellow | 2.08 | 42.27 | 20.32 | 1.024 | 0.203 |
| cadmium yellow | 1.84 | 21.06 | 11.45 | 0.921 | 0.196 |
| cinnabar | 2.50 | 88.01 | 35.20 | 1.351 | 0.171 |
| mars red | 1.73 | 16.71 | 9.66 | 0.504 | 0.179 |
| burnt sienna | 1.54 | 11.53 | 7.49 | 0.384 | 0.272 |
| cadmium red | 2.02 | 30.56 | 15.13 | 1.089 | 0.169 |
| alizarin carmine | 1.21 | 1.54 | 1.27 | 0.180 | 0.204 |
| silver white | 2.99 | 65.83 | 22.02 | 1.585 | 0.168 |
| burnt umber | 1.43 | 15.84 | 11.07 | 0.430 | 0.138 |
| Prussian blue | 1.23 | 6.66 | 5.41 | 0.135 | 0.169 |
| ultramarine | 1.40 | 4.09 | 2.92 | 0.217 | 0.209 |
| cobalt blue | 1.87 | 17.07 | 9.13 | 0.491 | 0.183 |
| chrome green | 1.41 | 14.43 | 10.23 | 0.348 | 0.201 |
| ivory black | 1.35 | | | 0.190 | 0.147 |
| white lead | 3.03 | 76.34 | 25.19 | 1.827 | 0.147 |
| massicot | 4.85 | 94.45 | 19.47 | 1.973 | 0.144 |
| Naples yellow | 3.67 | 74.07 | 20.18 | 1.973 | 0.154 |
| carbon black | 1.49 | 0.77 | 0.52 | 0.430 | 0.111 |
| azurite | | 32.06 | | 0.994 | 0.193 |
| copper acetate | | 21.14 | | 0.988 | 0.101 |

TABLE 1 Colours applied on a white industrial preparation (colour in tubes)
Source: ENEA

called photographic density, which is measurable by means of optical instruments [7]. For relatively simple paint layers, and in absence of complex stratifications, calibration of reference samples may be useful to read a radiographic image in order to check its composition. The impossibility of directly evaluating the radiopacity of a pigment by simply measuring the grey level on an x-ray plate is clear, the parameters are many and not all directly controllable as, e.g., the nature of the support and of the preparation, the variation in thickness. Moreover, generally pigments are almost never employed as pure, but in mixtures, and various layers of different composition are superimposed.

However, it is possible to perform a calibration carrying out measurements on specially-made samples. The data obtained in this way can be compared with those calculated through the above formulas.

The possibility of measuring the radiopacity of each paint layer is based on the following findings. Suppose that the paint layer is superimposed on other homogeneous layers (i.e., the preparatory ones). If we measure, on the radiographic film, the grey levels in this coloured area as well as outside it, where the paint layer is interrupted, and not the underlying ones, we can evaluate the contribution of the underlying layer. On the basis of the above considerations, reference

| | ρ | μ | S | R | σ |
|------------------|--------|-------|-------|-------|----------|
| yellow ochre | 1.58 | 8.02 | 5.08 | 0.350 | 0.216 |
| natural sienna | 1.46 | 10.36 | 7.10 | 0.302 | 0.195 |
| cinnabar | 2.50 | 88.01 | 35.20 | 1.361 | 0.201 |
| mars red | 1.73 | 16.71 | 9.66 | 0.639 | 0.251 |
| burnt sienna | 1.54 | 11.53 | 7.49 | 0.570 | 0.264 |
| alizarin carmine | 1.21 | 1.54 | 1.27 | 0.248 | 0.292 |
| burnt umber | 1.43 | 15.84 | 11.07 | 0.771 | 0.241 |
| ultramarine | 1.40 | 4.09 | 2.92 | 0.305 | 0.250 |
| white lead | 3.10 | 76.78 | 24.77 | 2.422 | 0.206 |
| massicot | 4.43 | 93.06 | 21.01 | 2.664 | 0.173 |
| Naples yellow | 3.35 | 71.20 | 21.25 | 2.464 | 0.178 |
| carbon black | 1.45 | 0.77 | 0.53 | 0.737 | 0.170 |
| nero d'avorio | 1.35 | | | 0.470 | 0.220 |
| copper acetate | | 20.84 | | 1.159 | 0.185 |
| azurite | | 32.06 | | 1.260 | 0.259 |

TABLE 2 Colours applied on a brown preparation (colour in tubes)
Source: ENEA

| | ρ | μ | S | R | σ |
|------------------|--------|--------|-------|-------|----------|
| yellow ochre | 1.53 | 8.32 | 5.44 | 0.737 | 0.292 |
| natural sienna | 1.28 | 8.38 | 6.55 | 0.381 | 0.313 |
| cinnabar | 2.85 | 118.83 | 41.69 | 1.916 | 0.236 |
| natural sienna | 1.36 | 11.71 | 8.61 | 0.753 | 0.362 |
| alizarin carmine | 1.10 | 0.88 | 0.80 | 0.356 | 0.470 |
| burnt umber | 1.33 | 13.94 | 10.48 | 0.463 | 0.301 |
| ultramarine | 1.12 | 2.89 | 2.58 | 0.185 | 0.402 |
| white lead | 2.00 | 61.66 | 30.83 | 2.205 | 0.273 |
| Naples yellow | 2.25 | 59.54 | 26.46 | 1.604 | 0.312 |
| carbon black | 1.20 | 0.78 | 0.65 | 0.411 | 0.435 |
| ivory black | 1.31 | | | 0.309 | 0.310 |
| copper acetate | | 17.08 | | 0.694 | 0.454 |

TABLE 3 Colours applied on a brown preparation (raw pigments and linseed oil)
Source: ENEA

standards have been performed in laboratory with the following modalities: canvas sizing using rabbit skin glue, homogeneous preparation having known composition and thickness, and paint layers with known and constant thickness.

Different types of preparatory layers were taken into account. In particular earth-based preparations using powdered pigments and linseed oil; the same kind of preparation made with ready colours in tubes; white industrial preparations.

For the paint layers, both ready-prepared colours in tubes and powder pigments mixed with known amounts of linseed oil were used. All of them were applied with a silk screen technique, in order to obtain a uniform thickness for all the samples. Moreover, a series of samples was realized with three superimposed layers, so as to verify their behaviour at different thicknesses, and their saturation conditions due to the layer thickness.

Optical Attenuation on Radiographs and Calculation of Absorption Coefficients

For each sample the mass absorption coefficients were calculated, taking into account the quantities of oil medium. For tube colours we considered the composition declared by the manufacturer, taking into account also the presence of filler materials. The densities (ρ) were experimentally measured. For pigments obtained from natural mixtures, the compositions declared in handbooks were used [8-10]. The canvases, prepared as described above, were radiographed using an x-ray generator set to 20 kV and 5 mA.

On the radiographs of each canvas ten attenuation measurements were performed on the coloured areas and on the surrounding preparation, in order to minimize the effects due to inhomogeneities in the paint layer and in the preparation. The mean value and the standard deviation for each group of measurements were calculated. The difference between the mean values measured on each coloured area and on the preparation provides the attenuation due to paint layer alone.

Tables 1-4 show the values for the densities (ρ), the absorption coefficients (μ and S), and the mean value of the optical attenuation (R) for each paint layer and the related standard deviation (σ).

Only in quite simple cases can the contribution of a paint layer be separated from the contribution of the underlying ones, maintaining a good correlation between the optical attenuation measured, and the attenuation coefficient calculated for the corresponding pigment. However, this operation is affected by high measurement errors.

| | 1 layer R σ | 2 layers R σ | 3 layers R σ |
|------------------|--------------------|---------------------|---------------------|
| yellow ochre | 0.350 0.216 | 0.752 0.185 | 0.984 0.192 |
| natural sienna | 0.302 0.195 | 0.572 0.183 | 0.798 0.200 |
| cinnabar | 1.361 0.201 | 2.060 0.193 | 2.226 0.187 |
| mars red | 0.639 0.251 | 1.046 0.236 | 1.355 0.242 |
| burnt sienna | 0.570 0.264 | 0.939 0.239 | 1.323 0.230 |
| alizarin carmine | 0.248 0.292 | 0.412 0.246 | 0.403 0.243 |
| burnt umber | 0.520 0.216 | 0.848 0.209 | 1.102 0.212 |
| ultramarine | 0.246 0.213 | 0.520 0.211 | 0.687 0.204 |
| white lead | 2.422 0.206 | 2.702 0.166 | 2.728 0.165 |
| massicot | 2.664 0.173 | 2.719 0.165 | 2.715 0.166 |
| Naples yellow | 2.464 0.178 | 2.685 0.166 | 2.722 0.165 |
| carbon black | 0.737 0.170 | 1.088 0.153 | 1.364 0.163 |
| ivory black | 0.470 0.220 | 0.674 0.210 | 0.879 0.211 |
| copper acetate | 1.159 0.185 | 1.749 0.333 | 1.887 0.150 |

TABLE 4 Colours applied in three layers on a brown preparation (colours in tubes)
Source: ENEA

XRF Analysis

The XRF (x-ray fluorescence) analysis is a non-destructive technique, which can supply information about the elemental composition of the matters employed on a painting, as it does not require the taking of samples, and an unlimited number of points can be observed.

This technique allows for the elemental semi-quantitative evaluation of all the chemical elements having an atomic number equal to or greater than 20 (i.e., from calcium upwards) [11-12]. It is therefore possible to obtain an indirect identification or characterisation of the mineral compounds/pigments through the detection of heavy elements present in the composition of each observed point as macro- or micro-constituents.

Unfortunately, the impossibility to detect elements with low atomic number does not allow to observe pigments containing only light elements, such as lapis lazuli or organic pigments (red lakes, etc.). For a correct interpretation of the XRF results, it is very important to remember this impossibility. Moreover, the obtained results involve all painting layers,



FIGURE 1 The Trivulzio portrait during the execution of the XRF measurements
Source: ENEA



FIGURE 2 Investigated areas enhanced on the radiograph
Source: ENEA and Opificio delle Pietre Dure (OPD)

reaching the support.

At the laboratories of the ENEA Casaccia Research Centre, XRF analysis on paintings has been carried out since 1988. At present, our digital archives contain more than 100,000 spectra referring to about 1,500 works of art, taken with the same XRF system, specifically designed for this purpose, and in the same operative conditions. The XRF system is formed by an x-ray generator Gilardoni CPX-M160 and a Ge(hp) planar detector EG&G ORTEC, having resolution 195 eV at 5.9 keV. The distance sample-detector is 6.5 cm, 0.1 cm the collimation diameter on the incident x beam, 180 seconds the time of each measurement, 4.0 mA the current, while for high voltage two different conditions (60 kV and 20 kV) are generally used. The second condition is adopted in order to better detect all the elements having fluorescence lines with lower energy. In the first condition the incident x beam is shielded, in front of the collimator, with a copper foil 0.05 cm thick, in order to attenuate the low energy component.

A Case Study

As an application example, the model was applied to the

Trivulzio portrait by Antonello da Messina, belonging to the Civic Museum of Ancient Art in Palazzo Madama (Turin) [13]. The choice of this painting for testing the model was justified by the exceptional thinness of the paint layers and of the panel support, and by the simple and concentrated palette, which determines homogeneity without creating interferences and uncontrolled fluctuations. XRF measurements (Figs. 1, 2) were carried out on 6th May, 2005, at the Opificio delle Pietre Dure in Florence, during the painting restoration; the painting was radiographed by Alfredo Aldrovandi of the Opificio delle Pietre Dure with the following operative parameters: high voltage 32 kV, current 5 mA, exposition time 5 minutes, distance between the x-ray tube and the painting 220 cm.

The relatively low intensities of the fluorescence lines of all the detected elements for this painting ensure that we were far from saturation conditions. The photographic density of each zone investigated by the XRF analysis was measured on the films through an optical densitometer.

Since the photographic density is related to the composition of the material, a multiple linear regression was conducted using the photographic density (D) as

the dependent variable, and the measured intensities of the fluorescence lines for the various elements as the independent variables. Manganese, calcium and strontium were not considered, the former because it has only been detected twice as a trace, the other two latter elements because they are linked to the composition of the preparatory layers. For this reason, the intensities of their fluorescence lines (which would be almost constant, with no real influence on photographic density) are affected from shield effects by the paint layers, which vary with the colour and the stratigraphy of the zone investigated. The multiple regression obtained is represented by the following formula, whose coefficients are shown in Table 5, whereas Fe, Cu, Hg, Pb, Sn are the intensities of the fluorescence lines of the elements.

$$D = A_0 + A_{Fe} * Fe + A_{Cu} * Cu + \\ + A_{Hg} * Hg + A_{Pb} * Pb + A_{Sn} * Sn$$

From the analysis of the data supplied from the regression, it is evident that the greatest contribution to photographic density is supplied by the wood panel and preparatory layers, which are nearly homogeneous over the entire surface, and which are represented by the constant factor in the formula for linear regression (A_0). As a higher shield causes a lighter areas on the plate, which in turn corresponds to smaller values of photographic density, the contribution to the regression by the five considered elements is systematically negative, so that the values of their respective coefficients are also negative. It is interesting to observe the effects of the individual elements on the changes in photographic density is represented by the absolute value of the respective coefficients. The lowest coefficient is related to the iron which is contained in pigments less radiopaque than those containing the other elements taken into account by the regression, such as copper, mercury, tin or lead.

The value for the tin coefficient is higher than those for mercury and lead, because the regression data used refer to different lines (K lines for tin and L lines for mercury and lead), which have markedly different fluorescence yields. It should be noted however that in XRF measurements on the *Trivulzio portrait* the presence of tin was determined only twice, on the

| | |
|----------|------------|
| A_0 | 3,055 |
| A_{Fe} | -2,581E-04 |
| A_{Cu} | -2,501E-03 |
| A_{Hg} | -6,553E-03 |
| A_{Pb} | -7,733E-03 |
| A_{Sn} | -1,186E-02 |

TABLE 5 Coefficients of multiple regression analysis relating the measured photographic density on the radiographic films to the XRF measurements
Source: ENEA

baluster in front of the sitter (points 2 and 3). On the other hand, the proximity of the values for the coefficients of mercury and lead is to be expected, especially considering the proximity of their respective coefficients of mass absorption, according to which it is possible to calculate the radiopacity of the pigment, estimated by A. Martin De Wild for white lead (88.5 cm²/gr for the pure pigment and 70.9 cm²/gr for the pigment with oil) and cinnabar (81.7 cm²/gr for the pure pigment and 72.7 cm²/gr for the pigment with oil).

As a check for the quality of the regression (with

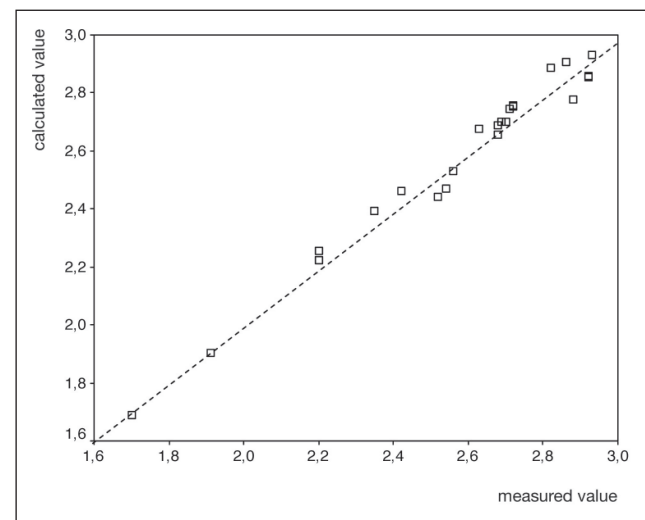


FIGURE 3 Comparison between the values of the photographic density measured on the radiographic film and the calculated ones from the multiple regression
Source: ENEA

a correlation coefficient $r=0.989$) the density values measured on photographic plates were compared with those calculated from the XRF data on the basis of the multiple regression (Fig. 3). The high correlation demonstrates the correctness of the physical model, and the absence of any saturation effects attributable to thick, or too rich and complex stratifications, which would have involved shield effects on the contributions of some elements, differing from point to point, depending on the composition and the stratigraphic succession of the various levels.

As shown in Fig. 3, differences between the calculated and measured values can be seen where the intensity of the lines of the various elements are smaller, due to measurement errors. However, if we calculate residual values, i.e., the differences between the value calculated and measured at each point, we still have a normal distribution with mean value equal to 0.0 and standard deviation equal to 0.88.

The major differences are observed for some points with higher values of photographic density, but the fact that these areas are those related to the maximum dark provides a physical justification for these discrepancies. In fact, the photographic density of these areas scarcely affects the factors taken into account in the regression, while the XRF analysis gives no information on the elements with low atomic number contained in the dark pigments used, probably based on carbon blacks. On the other hand, the photographic density fluctuations in the darker areas, due to the contribution of the preparatory layers and the panel grain, and consequently the increasing in the standard deviation values appreciably affect the difference between the measured value and that calculated on the basis of the specific XRF analysis.

Conclusions

In this paper we have tried to verify – on theoretical grounds, then experimentally on appositely executed standards and, finally, on a real painting – the effective correlation subsisting between two physical quantities related to the density and composition of matter. This verification was performed by using

quantitative parameters derived from non-destructive techniques of investigation, usually performed in the diagnostics of paintings: x-radiography and XRF analysis. The results obtained are encouraging. In fact, the high correlation reached for the data related to the *Trivulzio portrait* by Antonello da Messina, through the evaluation of the grey levels measured on the x-ray plate, allows to extrapolate the compositional results supplied from the XRF also in adjacent areas, where XRF measurements were not performed. In the future, we shall apply this method to other paintings.

Acknowledgements

We would like to thank Alfredo Aldrovandi, Roberto Bellucci, Marco Ciatti and Cecilia Frosinini of the Opificio delle Pietre Dure in Florence.

References

- [1] W.H. McMaster, N. Kerr Del Grande, J. H. Mallett, J. H. Hubbel (1969), *Compilation of X-Ray Cross Sections*, Lawrence Radiation Laboratory, University of California, UCRL-50174 Sec. II Rev. I.
- [2] A.M. De Wild (1929), *The scientific Examination of Pictures*, G. Bell & Sons Ltd., London.
- [3] A. Gilardoni, R. Ascani Orsini, S. Taccani (1977), *X-rays in Art*, Gilardoni, Como.
- [4] L. Paderni (1983), "I raggi X nell'arte", 1st International Conference on "Non-destructive Testing, Microanalytical Methods and Environment Evaluation for Study and Conservation of Works of Art" (Rome, 27-29 October 1983), I/21.1-13.
- [5] M. Matteini, A. Moles (1985), *Scienza e Restauro, Metodi di indagine*, Nardini Editore, Florence.
- [6] P. Moioli, C. Seccaroni (2004), *Tecniche radiografiche applicate ai Beni Culturali*, ENEA, Rome, pp. 29-53.
- [7] G. Accardo, P. Moioli, C. Seccaroni (1992), "Taratura di lastre radiografiche per analisi di dipinti", 3rd International Conference on "Non-destructive testing, microanalytical methods and environment evaluation for study and conservation of works of art" (Viterbo, 4-8 October 1992), pp. 21-35.
- [8] *Artists' Pigments*, voll. 1 (1985), 2 (1993), 3 (1997), 4 (2007).
- [9] N. Eastough, V. Walsh, T. Chaplin, R. Siddal (2004), *Pigment Compendium, A Dictionary of Historical Pigments and Optical Microscopy of Historical Pigments*, Elsevier Butterworth-Heinemann.
- [10] R.J. Gettens, G.L. Stout (1966), *Painting Materials. A Short Encyclopaedia*, New York 1966.
- [11] P. Moioli, C. Seccaroni (1999), "Analysis of Art Objects Using a Portable X-Ray Fluorescence Spectrometer", *X-Ray Spectrometry*, vol. 29 n. 1, pp. 48-52.
- [12] P. Moioli, C. Seccaroni (2002), *Fluorescenza x. Prontuario per l'analisi XRF portatile applicata a superfici policrome*, Nardini Editore, Florence.
- [13] R. Bellucci, P. Bonanni, B.G. Brunetti, S. Calvi, C. Castelli, M. Cianfanelli, M. Ciatti, B. Doherty, R. Fontana, C. Frosinini, L. Giuntini, N. Grassi, P.A. Mandò, M. Massi, M. Mastroianni, M. Materazzi, A. Migliori, C. Miliani, P. Moioli, E. Pampaloni, L. Pezzati, P. Pingi, F. Rosi, C. Seccaroni, F. Seracini, A. Sgamellotti (2010), "Il restauro del Ritratto Trivulzio di Antonello da Messina", *OPD Restauro*, 22, pp. 15-54. [P. Moioli, C. Seccaroni, *Le analisi XRF*, pp. 43-52].